Journal of Archaeological Science: Reports 5 (2016) 392–399

Contents lists available at ScienceDirect

Journal of Archaeological Science: Reports

journal homepage: www.elsevier.com/locate/jasrep

Characterization of obsidian from the Tibetan Plateau by XRF and NAA

Charles Perreault [a,b,*], Matthew T. Boulanger [c], Adam M. Hudson [d], David Rhode [e], David B. Madsen [f], John W. Olsen [g], Martina L. Steffen [g], Jay Quade [d], Michael D. Glascock [h], P. Jeffrey Brantingham [i]

[a] School of Human Evolution and Social Change, Arizona State University, PO Box 872402, Tempe, AZ 85287-2402, USA
[b] Institute of Human Origins, Arizona State University, PO Box 874101, Tempe, AZ 85287, USA
[c] Department of Anthropology, Southern Methodist University, P.O. Box 750336, Dallas, TX 75275, USA
[d] Department of Geosciences, University of Arizona, 1040 E. 4th Street, Tucson, AZ 85721, USA
[e] Division of Earth and Ecosystem Sciences, Desert Research Institute, 2215 Raggio Parkway, Reno, NV, USA
[f] Department of Anthropology, Texas State University, Evans Liberal Arts 266, 601 University Drive, San Marcos, TX 78666-4684, USA
[g] School of Anthropology, University of Arizona, P.O. Box 210030, Tucson, AZ 85721-0030, USA
[h] Archaeometry Laboratory, University of Missouri Research Reactor, 1513 Research Park Drive, Columbia, MO 65211, USA
[i] Department of Anthropology, University of California, Los Angeles, 341 Haines Hall, Los Angeles, CA 90095, Box 951553, USA

ARTICLE INFO

Article history:
Received 15 June 2015
Received in revised form 24 November 2015
Accepted 11 December 2015
Available online 22 December 2015

Keywords:
Tibet
Archeology
High altitude adaptation
Human expansion
Obsidian characterization
Mobility
Lithic raw material transportation distances

ABSTRACT

The Tibetan Plateau is the highest contiguous terrain on the planet. It is cold, dry, poor in oxygen, and one of the last habitats to have been colonized by our species. Here we present the first quantitative chemical characterization of obsidian artifacts from the Tibetan Plateau. The artifacts in our sample come from 20 archeological sites spanning a large portion of the northeast and the southwest regions of the Plateau. We find that five varieties of obsidian were used at these sites. We also identify the geological source of one of the obsidian varieties as near Balung Tso in south-central Tibet. The five varieties of volcanic glass are distributed into two discrete zones in the northeast and the southwest of Tibet, suggesting that the two regions may have been occupied independently, and that interactions between them were limited. Finally, we also find that some of the transportation distances of obsidian are several hundred kilometers long.

1. Introduction

The Tibetan Plateau contains the world's highest mountains and the largest contiguous land area exceeding 4000 masl. The combination of high altitude, cold temperatures, and low rainfall in the rain shadow of the Himalayan ranges creates a harsh environment for human habitation (Aldenderfer and Zhang, 2004, Beall et al., 2004, Brantingham et al., 2007). Indeed, archeological evidence indicates that it is one of the last habitats to have been colonized by our species.

By at least 34 kya, modern humans occupied the low-elevation areas that surround the northern part of the Tibetan Plateau (Barton et al., 2007, Brantingham et al., 2004, Gao et al., 2004, Ji et al., 2005, Li et al., 2013, Madsen et al., 2001, Madsen et al., 2014). Yet, the high-elevation areas of the Plateau (>4000 masl) remained uninhabited until the early Holocene (Brantingham and Xing, 2006, Brantingham et al., 2013, Brantingham et al., 2007). The oldest evidence of human presence above 4000 masl dates to ~11,300 cal. year BP (Brantingham et al., 2013, Brantingham et al., 2007, Van Der Woerd et al., 2002), and year–round occupation above 3000 masl likely postdates 7000 years BP, when Epipaleolithic foragers that interacted with Neolithic populations from the periphery began to hunt on the high Plateau (Brantingham et al., 2013, Brantingham et al., 2007, Chen et al., 2015, Rhode et al., 2007). This is in contrast to the colonization of high elevation areas in the central Andes by 12,400 years BP, at most only 2000 years after the earliest evidence of the arrival of *Homo sapiens* in South America (Rademaker et al., 2014).

Why did it take 20 thousand years for humans to exploit the Tibetan Plateau? The answer to this question lies in part in the fact that the high, flat interior of the Plateau constitutes a formidable biogeographic barrier. By comparison to the central Andes where the maximum distance across the high-elevation cordillera is less than 300 km, the Tibetan Plateau cordillera at its narrowest point exceeds 300 km and at its widest is more than 1000 km. Procuring raw material from the geological sources considered here requires a minimum of ~360 km round-trip travel from any location below 4000 masl. Humans are not preadapted to life at high altitude, which presents an impediment to even seasonal occupations at high-altitude. Present-day Tibetans possess a suite of physiological adaptations (Beall, 2007, Beall et al., 2010, Chen et al., 1997, Ge et al.,

* Corresponding author at: School of Human Evolution and Social Change, Arizona State University, PO Box 872402, Tempe, AZ 85287-2402, USA.
E-mail address: cperreault@asu.edu (C. Perreault).

http://dx.doi.org/10.1016/j.jasrep.2015.12.009
2352-409X/

2002, Ge et al., 1994, Groves et al., 1993, Simonson et al., 2010, Wang et al., 2011, Yi et al., 2010), that allows them to live in high-elevation regions. What remains unclear, however, is the timing of the appearance of these adaptations, as well as the amount of time it took for them to emerge (Brantingham et al., 2010, Yi et al., 2010).

In addition to physiological changes, behavioral adaptations may have been required to occupy the Plateau. Could the lack of such behavioral adaptations further impede the exploitation of Tibet, above and beyond the necessity of biological adaptations? A recent model of the human presence in Tibet emphasizes the role of an agropastoral economy based first on millet (5200 years BP) and then on barley (3600 years BP) in facilitating year-long occupation of the Plateau (Chen et al., 2015). This model, however, does not account for the presence of human foragers before 5200 years BP. Special behavioral adaptations from foragers may have been needed to occupy high-altitude environments, such as Tibet, that are characterized by unusually low environmental productivity and patchy unpredictable distributions of food resources (Aldenderfer and Zhang, 2004, Yang et al., 2009).

Given that the majority of archeological artifacts dating to the Epipaleolithic and Neolithic on the Tibetan Plateau consist of stone tools and debitage, analyses aimed at documenting the transportation of lithic raw material have the potential to open a window onto the behavioral adaptations that accompanied the colonization of the Plateau. Studies of the sources of lithic artifacts on the Plateau are in their infancy, and those data that do exist have been drawn from limited analyses of obsidian artifacts. Here we present the first quantitative chemical characterization of obsidian artifacts from the Tibetan Plateau. Previous discussions on the use of obsidian artifacts from Tibet (Brantingham et al., 2013, Rhode et al., 2007), have provided limited presentation of archaeometric data for those artifacts. We present here chemical characterization data for a sample of obsidian artifacts and one source nodule from Tibet. Our findings suggest that (1) prehistoric populations in Tibet exploited at least five sources of volcanic glass and that (2) several of the lithic-raw-material transportation distances observed in Tibet are hundreds of kilometer long, which makes them comparable to some of the longest transportation distances observed in other parts of the world.

2. Study sites and materials

Obsidian is rare compared to other lithic materials at archeological sites in Tibet. Most of the stone artifacts discovered at the sites discussed here are visually consistent with cryptocrystalline silicates[1] (e.g., chert). However, obsidian sources tend to exhibit distinctive chemistries, making the identification of sources a process that is usually straightforward. This is not to say that chemical analyses of the (presumably) chert artifacts and source materials should not be undertaken—far from it. We have simply chosen to limit our sample to volcanic glass specimens because of the limited number of geological sources assumed to exist across the Plateau, and the high degree of potential confidence in identifying these.

Forty-seven volcanic-glass artifacts were chemically characterized (Table 1). The artifacts represent microlithics (e.g., microblades and microblade cores) as well as generalized unifacial and bifacial flake technologies. Our sample is necessarily limited by the small number of specimens available for analysis; yet, to the best of our knowledge it is the largest sample of obsidian artifacts—and the only chemical analysis of a source nodule—yet analyzed for this vast region. The specimens were obtained from archeological sites in two different regions of the Tibetan Plateau (see Fig 1) The sites are separated by significant geographic distances and changes in altitude. To address these geographic factors, we group the sites into two general regions: Southwest and Northeast. The northeastern specimens ($n = 13$) were collected from the central and northeastern Tibetan Plateau. Four of these sites are

Table 1
Specimens of obsidian analyzed. The ID number refers to the specimen ID used in the Supplemental Information.

Region	Site	Longitude	Latitude	Altitude	ID	Description
Northeast	Erdaogou	92.82	34.63	4765	2	Microblade core
Northeast	Jiangxigou 2	100.3	36.59	3312	3	Flake
Northeast	Jiangxigou 2	100.3	36.59	3312	4	Shatter
Northeast	Lava Camp	89.358	34.529	4880	5	Flake
Northeast	Lava Camp	89.358	34.529	4880	6	Flake
Northeast	Lava Camp	89.358	34.529	4880	20	Scraper
Northeast	Lava Camp	89.358	34.529	4880	21	Flake
Northeast	Lava Camp	89.358	34.529	4880	22	Flake
Northeast	Lexie Wudan Co	90.14	35.48	4913	23	Microblade core
Northeast	Police Station 1	93.61	35.43	4451	1	Core
Northeast	Xidatan 2	94.26	35.7	4300	7	Scraper
Northeast	Xidatan 2	94.26	35.7	4300	8	Flake
Northeast	Xidatan 2	94.26	35.7	4300	9	Flake
Southwest	Balung Co 13–23	83.528	30.59	5266	17	Flake
Southwest	Balung Co 13–23	83.528	30.59	5266	46	Large flake/scraper
Southwest	Balung Co 13–3	83.615	30.805	5165	48	Unworked cobble
Southwest	Kay Lak 11–3	83.438	30.361	4670	18	Flake
Southwest	Kay Lak 11–4	83.444	30.36	4670	16	Core
Southwest	Kay Lak 11–7	83.328	30.339	4645	13	Flake
Southwest	Kay Lak 11–7	83.328	30.339	4645	14	Flake
Southwest	Kay Lak 11–7	83.328	30.339	4645	15	Flake
Southwest	Kay Lak 11–7	83.328	30.339	4645	43	Large flake/scraper
Southwest	Lopu Kangri 11-9A	84.453	29.981	5326	41	Flake
Southwest	Lopu Kangri 13–1	84.224	29.864	4722	44	Large flake/scraper
Southwest	Lopu Kangri 13–1	84.224	29.864	4722	45	Large flake/scraper
Southwest	Ngangla Ring Co 10–12	82.583	31.658	4790	11	Flake
Southwest	Ngangla Ring Co 10–14	82.59	31.659	4801	19	Microblade core
Southwest	Ngangla Ring Co 10–4	83.357	31.198	4848	10	Wedge
Southwest	Ngangla Ring Co 10–7	82.692	31.684	4872	12	Flake
Southwest	Paiku Co 2	85.53	28.857	4658	36	Microblade core
Southwest	Paiku Co 2	85.53	28.857	4658	37	Flake
Southwest	Paiku Co 2	85.53	28.857	4658	38	Flake
Southwest	Paiku Co 3	85.506	28.831	4624	39	Flake
Southwest	Paiku Co 3	85.506	28.831	4624	40	Flake
Southwest	Su-Re	86.672	28.516	4453	24	Flake
Southwest	Su-Re	86.672	28.516	4453	25	Flake
Southwest	Su-Re	86.672	28.516	4453	26	Flake
Southwest	Su-Re	86.672	28.516	4453	27	Flake
Southwest	Su-Re	86.672	28.516	4453	28	Flake
Southwest	Su-Re	86.672	28.516	4453	29	Flake
Southwest	Su-Re	86.672	28.516	4453	30	Flake
Southwest	Su-Re	86.672	28.516	4453	31	Flake
Southwest	Su-Re	86.672	28.516	4453	32	Flake
Southwest	Su-Re	86.672	28.516	4453	47	Microblade core
Southwest	Tingri 1	86.571	28.62	4358	33	Microblade core
Southwest	Tingri 1	86.571	28.62	4358	34	Flake
Southwest	Tingri 1	86.571	28.62	4358	35	Flake
Southwest	Zhongba 13–3	84.169	29.664	4574	42	Microblade core

[1] For example, at Jiangxigou 2 the two obsidian specimens we analyzed were the only pieces of obsidian in an assemblage of 965 stone artifacts (Rhode et al., 2007). Jiangxigou 2 is the only site of at least 13 others in the Qinghai Lake area that we investigated thoroughly. Similarly, the three pieces of obsidian from Xidatan were the sole obsidian specimens among 172 stone artifacts (Brantingham et al., 2013). The situation is similar in the southwestern Plateau, although sites containing obsidian are more frequent there, perhaps indicating greater use of obsidian or greater proximity to source(s). Even so, the majority of artifacts identified in southwestern sites are derived from a variety of other lithic materials usually found cropping out within a few km of the sites.

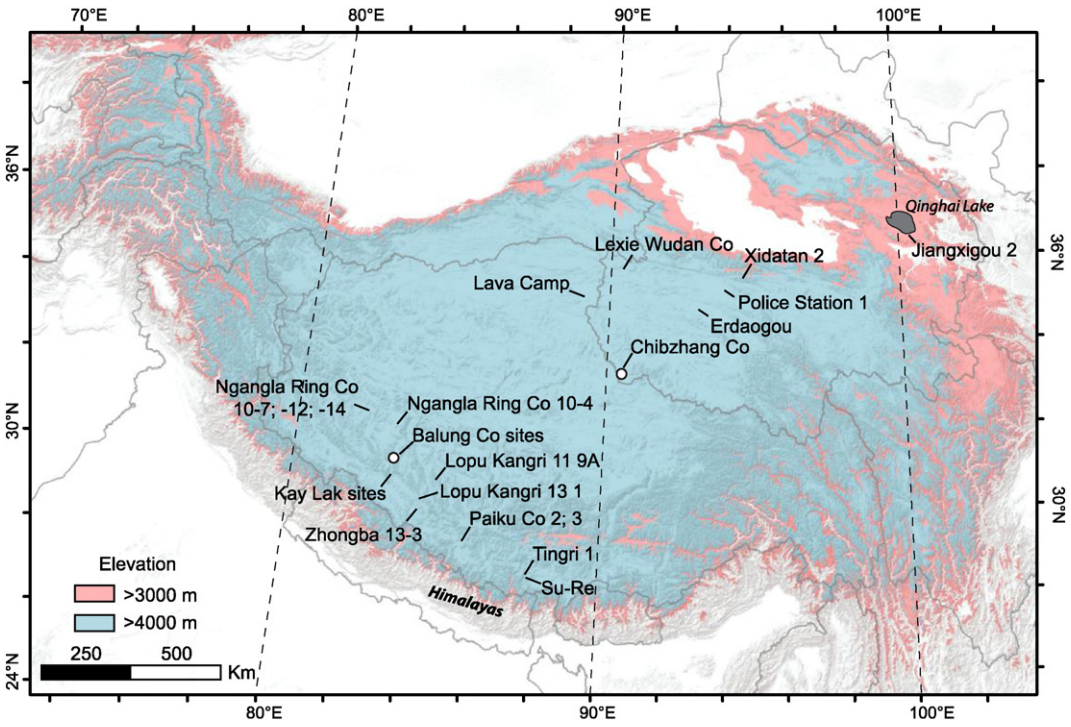

Fig. 1. Site locations of obsidian artifacts characterized described in the text. Chibzhang Co is the purported geological source of *Northeastern Obsidian A*, and one Balung Co site is the geological source of *Southwestern Obsidian D*.

located above 4000 masl, two are located on the shores of Qinghai Lake at 3312 masl. The southwestern specimens ($n = 34$) were collected from 15 sites located above 4000 masl adjacent to the China-Nepal border, along the northern foothills of the Himalayas.

The sites also come from a variety of environmental contexts. Several sites are located in lake basins: Jiangxigou 2, Lava Camp, and Lexie Wudan Co in the northeast, and the Ngangla Ring Co sites ($n = 4$), the Paiku Co sites ($n = 5$), the Balung Co locations ($n = 2$) in the southwest. In addition, from the northeast, Police Station 1 is in an open alpine steppe-meadow, Erdaogou is associated with a perennial stream, whereas Xidatan 2 is located in a glacial outwash terrace near the Kunlun Pass. In the southwest, the Kay Lak sites ($n = 5$) are in a fertile river valley, the two Lopu Kangri sites are in the glacial valleys of the Lopu Kangri range, Su-re (Shire in Mandarin Chinese) lie in a small branch of the Longjiang Valley, while the Zhongba site is located in a set of paleowetland deposits within eolian dunes of the Yarlung-Tsangpo floodplain.

With the exception of the specimens from Jiangxigou 2 and Xidatan 2, all of the artifacts reported here come from surface scatters. Some sites such as Lava Camp and several locations in the southwest region contained dozens of artifacts that appeared to be made of obsidian. Instead of analyzing every single one of these artifacts, we analyzed only a sample of them, making an effort to include specimens that were visually distinct. In addition, many of the specimens were collected in the context of reconnaissance survey, from sites that were not excavated in a systematic manner.

We have yet to determine the full temporal distribution of these artifacts, although a number of published radiometric dates indicate they are likely Holocene in age. Artifacts from the northeastern region appear to date from the early to middle Holocene. The material from Jiangxigou 2 is dated between 9140 ± 90 and 5580 ± 60 cal. years BP (Rhode et al., 2007), and that of Xidatan 2 to 9200–6400 years BP (Brantingham et al., 2013). Based on our current understanding of the prehistory of Tibet (Brantingham et al., 2013), we expect that the sample of artifacts from the northeastern region were produced between 12,000 and 5000 years ago, and probably by a mixture of late Upper Paleolithic foragers, Epipaleolithic foragers, and, potentially, Neolithic hunting parties and pastoralists (Rhode et al., 2007).

Artifacts from the southwestern region are believed to be slightly younger than those of the northeastern region, dating to between 8500 years BP and 1300 years BP. Although no obsidian artifacts from the southwestern region have direct age constraints, limiting ages for artifacts from Zhongba (where one *in situ* obsidian artifact was recovered) indicate that similar lithic technologies occurring in similar site contexts date to between 6590 ± 90 cal. year BP and 1310 ± 40 cal. year BP (Hudson et al., 2014). Similarly, all but one of the sites surrounding the Ngangla Ring Co paleolake (Ngangla Ring Co 10–4, 12, 14) are located well below the elevation of the high shoreline of the well-dated early Holocene deep lake interval (Hudson et al., 2015). These sites must certainly postdate the fall of the lake level from the maximum of 4862 masl after 8500 years BP, with the locations of sites 10–12 and 10–14 not exposed until after 6000 years BP.

In addition to the 47 artifacts, we analyzed a single unworked nodule of obsidian collected from the shoreline of Balung Co in the southwestern region. This nodule shows some degree of weathering on its exterior, and the source locality appears to be a secondary deposit of obsidian cobbles/nodules eroding from a primary geological deposit nearby.

3. Analytical protocol

The specimens were analyzed at the Archaeometry Laboratory of the University of Missouri Research Reactor (MURR). All specimens were analyzed using non-destructive energy-dispersive X-ray fluorescence (XRF). Following the XRF analyses, a subset of specimens was analyzed by neutron activation (NAA). The separate analyses are complementary to each other, with the former providing a rapid determination of 11 elements useful in discriminating between most known obsidian sources, and the latter providing characterizations of 34 different elements. Data for individual specimens are provided in the Supplementary Information and are also available via the MURR Archaeometry Laboratory's Web site (http://archaeometry.missouri.edu).

3.1. Energy-dispersive X-ray fluorescence (XRF) protocol

The specimens were analyzed using a Bruker Tracer III–V X-ray fluorescence spectrometer using standard protocols for the analysis of obsidian (Khazaee et al., 2011). The Tracer III–V uses a Rh-based X-ray tube operating at 40 kV, and a thermoelectrically-cooled silicon p–n diode detector. The Tracer III–V was calibrated using over 40 well-characterized obsidian specimens (Glascock and Ferguson, 2012). Mean elemental-abundance values from multiple characterization studies conducted by neutron activation analysis (NAA) and inductively coupled plasma-mass spectrometry (ICP-MS) were used for the obsidian calibration specimens. All of the specimens from Tibet were analyzed on the Tracer III–V for at least three minutes. This protocol allowed for the quantification of minor and trace elements potassium (K), titanium (Ti), manganese (Mn), iron (Fe), zinc (Zn), gallium (Ga), rubidium (Rb), strontium (Sr), yttrium (Y), niobium (Nb), thorium (Th), and zirconium (Zr).

3.2. Neutron activation analysis (NAA) protocol

A subset of 14 specimens (ID # 3, 8, 9, 12, 13, 14, 15, 17, 20, 21, 23, 24, 25 and 26) were analyzed by NAA using standard procedures involving two irradiations and three gamma-ray counts (Glascock, 1992, Glascock and Neff, 2003, Neff, 2000). Crushed fragments of the specimen were weighed into two aliquots. Aliquots of ca. 100 mg were placed in high-density polyethylene vials, and used for short irradiations. Aliquots of 250 mg were vacuum-sealed in high-purity quartz vials and used for the long irradiation.

The specimens in the polyvials were irradiated for 5 s by a neutron flux of 8×10^{13} n cm^{-2} s^{-1}. The 720-second count yielded gamma spectra containing peaks for aluminum (Al), barium (Ba), chlorine (Cl), calcium (Ca), dysprosium (Dy), potassium (K), Manganese (Mn), and sodium (Na).

The specimens encapsulated in the quartz vials were irradiated for 70 h at a neutron flux of 5×10^{13} n cm^{-2} s^{-1}. After being irradiated, the specimens decayed for seven days, and were counted for 1800 s using a high-resolution germanium detector. This middle count yielded determinations of barium (Ba), lanthanum (La), lutetium (Lu), neodymium (Nd), samarium (Sm), uranium (U), and ytterbium (Yb). After another three- or four-week decay, an 8500-second count was taken, yielding determinations of cerium (Ce), cobalt (Co), cesium (Cs), europium (Eu), iron (Fe), hafnium (Hf), rubidium (Rb), antimony (Sb), scandium (Sc), strontium (Sr), tantalum (Ta), terbium (Tb), thorium (Th), zinc (Zn), and zirconium (Zr).

4. Results

4.1. Chemical characterization

The results of the XRF and NAA analyses (Tables 2, 3, and Supplemental Information) demonstrate the presence of five varieties of volcanic glass in our sample. Because geological source localities for all but one of the obsidian varieties have not been firmly established, we refer to these varieties as *NE Obsidian A*, *NE Obsidian B*, *NE Obsidian C*, *SW Obsidian A*, and *SW Obsidian B*.

4.1.1. NE obsidian A

Nine specimens in our sample exhibit a chemical profile that we refer to here as *NE Obsidian A*. Relative to the other varieties of obsidian in Tibet, this obsidian is enriched in Mn, Rb, Br, Cs, Ta, and depleted in Ti, Fe, Sr, Zr, and Th. Visually, it ranges from clear and translucent, to black and semi-opaque, with occasional dark-green tints. The chemical composition of *NE Obsidian A* corresponds to the "Plateau Obsidian" of Brantingham et al. (2013) and Rhode et al. (2007). Though unconfirmed, it is suspected that the source locality for this obsidian lies near Chibzhang Co (Migriggyangzham Tso).

Table 2
Mean and standard deviation of element abundances as determined by XRF. Data at or below detection limits are indicated as "n.d.". The *SW Obsidian B* group includes an unworked cobble (ID 48). All data in parts per million (ppm) unless otherwise indicated.

Element	NE Obsidian A	NE Obsidian B	NE Obsidian C	SW Obsidian A	SW Obsidian B
n	9	1	3	28	7
K%	3.632 ± .054	3.682	1.814 ± .089	3.588 ± .208	3.475 ± .07
Ti	704 ± 192	730	6320 ± 360	625 ± 88	911 ± 87
Mn	653 ± 112	563	1209 ± 138	260 ± 60	361 ± 107
Fe%	0.815 ± .074	0.911	5.215 ± .247	0.677 ± .046	1.325 ± 110
Zn	118 ± 17	148	229 ± 22	63 ± 15	98 ± 16
Ga	27 ± 3	21	27 ± 5	23 ± 3	24 ± 3
Rb	831 ± 17	841	166 ± 9	439 ± 21	439 ± 20
Sr	1 ± 2	4.5	744 ± 41	181 ± 10	245 ± 22
Y	2 ± 3	n.d.	34 ± 4	7 ± 3	7 ± 2
Zr	45 ± 3	43	682 ± 16	124 ± 7	194 ± 6
Nb	32 ± 2	34	43 ± 2	24 ± 2	10 ± 1
Th	38 ± 5	42	32 ± 1	81 ± 6	61 ± 2

4.1.2. NE obsidian B

A single specimen in our sample exhibits a slightly different chemical composition from *NE Obsidian A*, and is thus referred to as *NE Obsidian B*. This chemical variety of obsidian shows slight enrichment in K, Th, and Zn, and is depleted in Mn, Sb, Sc, Ta, and Yb relative to *NE Obsidian A*. Visually, the *NE Obsidian B* specimen is black and semi-opaque, making it visually indistinguishable from those specimens classified as *NE Obsidian A*.

The precision and accuracy of our XRF analysis does not permit us to distinguish between *NE Obsidian A* and *NE Obsidian B* (Fig. 2); however, this appears to be a limitation of the standard MURR instrument calibration. That is, the major differences between *NE Obsidian A* and *NE*

Table 3
Mean and standard deviation of element abundances as determined by NAA. Data at or below detection limits are indicated as "n.d.". All data in parts per million (ppm) unless otherwise indicated.

Element	NE Obsidian A	NE Obsidian B	NE Obsidian C	SW Obsidian A	SW Obsidian B
n	4	1	3	5	1
Al%	7.75 ± .188	8.07	7.78 ± .321	7.09 ± .13	8.03
Ba	168 ± 21	228	1605 ± 38	265 ± 15	656
Br	0.83 ± 0.33	0.78	0.84 ± 0.24	n.d.	n.d.
Ce	22.9 ± 0.2	24.9	310.4 ± 5.2	67.2 ± 0.6	119.4
Cl	476 ± 67	598	786 ± 102	328 ± 41	469
Co	0.39 ± 0.02	0.35	11.85 ± 0.10	0.31 ± 0.02	3.56
Cs	215.5 ± 1.4	132.5	2.6 ± 0.2	86 ± 0.4	55.1
Dy	0.8 ± 0.07	0.62	5.54 ± 0.48	0.65 ± 0.37	1.94
Eu	0.06 ± 0.02	0.1	3.16 ± 0.06	0.25 ± 0.02	0.91
Fe%	.702 ± .005	.741	4.547 ± .041	.59 ± .003	1.263
Hf	1.8 ± 0.1	1.8	14.2 ± 0.2	5.9 ± 0.03	6.4
K%	3.28 ± 0.08	3.85	3.36 ± 0.21	4.18 ± 0.12	3.86
La	7.4 ± 0.1	8.2	161.5 ± 1.5	41.7 ± 0.2	60.8
Lu	0.83 ± 0.02	n.d.	0.29 ± 0.05	n.d.	0.41
Mn	754 ± 6	522	703 ± 6.1	222 ± 3	251
Na%	2.869 ± 0.02	2.82	2.647 ± 0.031	2.703 ± 0.049	3.27
Nd	12.1 ± 1.7	15.2	104.3 ± 2.6	22.01 ± 7.7	40.1
Rb	803 ± 5	794	155 ± 3	448 ± 2	456
Sb	0.65 ± 0.02	0.16	0.05 ± 0.02	0.59 ± 0.02	0.3
Sc	2.33 ± 0.02	1.79	8.58 ± 0.1	1.12 ± 0.00	3.45
Sm	4.4 ± 0.04	4.6	15.3 ± 0.3	4.1 ± 0.1	8.2
Sr	n.d.	n.d.	850 ± 13	205 ± 9	345
Ta	9.64 ± 0.04	7.91	1.96 ± 0.03	1.75 ± 0.02	0.92
Tb	0.17 ± 0.02	0.17	1.19 ± 0.03	0.09 ± 0.01	0.28
Th	7.5 ± 0.2	10.5	32 ± 0.5	79.7 ± 0.4	66.4
U	41.3 ± 0.4	40.4	4.8 ± 0.5	28.7 ± 0.5	23.6
Yb	0.81 ± 0.03	0.23	1.77 ± 0.05	0.35 ± 0.05	0.61
Zn	79 ± 2	106	139 ± 4	35 ± 0.77	72
Zr	361 ± 11	349	611 ± 21	10	387

Obsidian B lie in the concentrations of Th and Mn. Regarding Th, the XRF calibration is incapable of accurately determining concentrations below ca. 40 ppm. Regarding Mn, the instrumental error appears to be too great to distinguish between the ca. 230 ppm difference between the two obsidian compositions. Differences between these obsidian varieties are apparent, however, in the NAA data (Figs. 3–5). Previous analyses using XRF have concluded that a single chemical variety of obsidian is present at sites on the northeastern Plateau (e.g. Brantingham et al., 2013, Rhode et al., 2007).

Generally speaking, *NE Obsidian A* and *NE Obsidian B* exhibit similar chemical compositions, perhaps an indication that these two varieties of obsidian are derived from the same magma pool. If this were the case, it would suggest that the geological sources for these glasses are located in close proximity.

4.1.3. NE obsidian C

Three specimens of volcanic glass, all obtained from the site of Lava Camp in the Northeastern region, are chemically distinct from the previous two varieties of obsidian identified from sites in the Northeast. This particular glass is enriched in nearly all elements—especially transition metals and rare earth elements. As with all of the varieties of obsidian identified in our sample of artifacts from northeastern sites, the geological source locality for this material is as-yet unknown. However, we note that this Fe-enriched glass was identified only within the assemblage from Lava Camp, perhaps suggesting that the source may be located nearby.

4.1.4. SW obsidian A

The two remaining obsidian varieties are distinct in both our XRF and our NAA data and appear to be visually distinctive. *SW Obsidian A* (n = 28) is enriched in K, Th, and Zr, and it is depleted in Co, Fe, Mn, Tb, Ti, and Zn. Visually, it varies from translucent to semi-opaque, with occasional banding of black and dark gray.

4.1.5. SW obsidian B

SW Obsidian B (n = 6) is enriched in Ba, Ce, Co, Dy, Fe, Ti, Si, Sr, Zr, and is depleted in Rb and U. Our specimens are black and semi-opaque, with a granular groundmass exhibiting numerous phenocrysts of conspicuous flow-aligned biotite. As mentioned above, one geological nodule of obsidian was collected from Balung Co, and analysis of this nodule reveals that it is of the same chemical makeup as the artifacts we have classified as *SW Obsidian B*. Because obsidian cobbles and pebbles appear in abundance in the alluvial fan adjacent to the lake, it seems reasonable to conclude that the primary geological source locality of *SW Obsidian B* exists in close proximity to Balung Co.

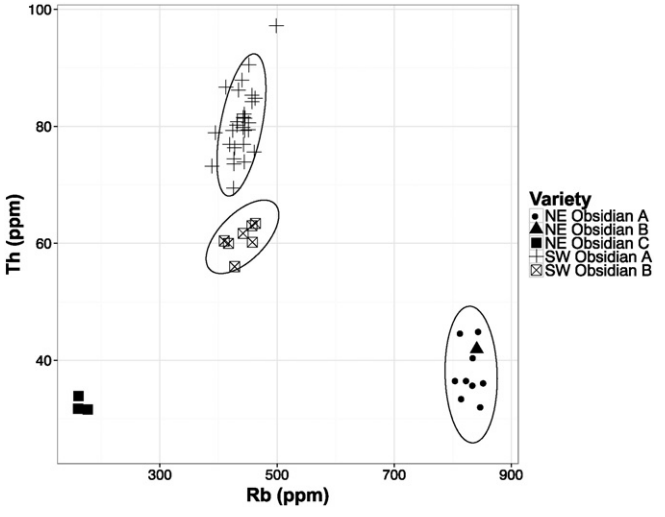

Fig. 2. Bivariate plot of Rb and Th abundances as determined by XRF. Ellipses drawn at the 95% confidence interval around obsidian sources *NE A*, *SW C* and *SW D*. Notice that source *NE B* cannot be discriminated from source *NE A* with XRF data.

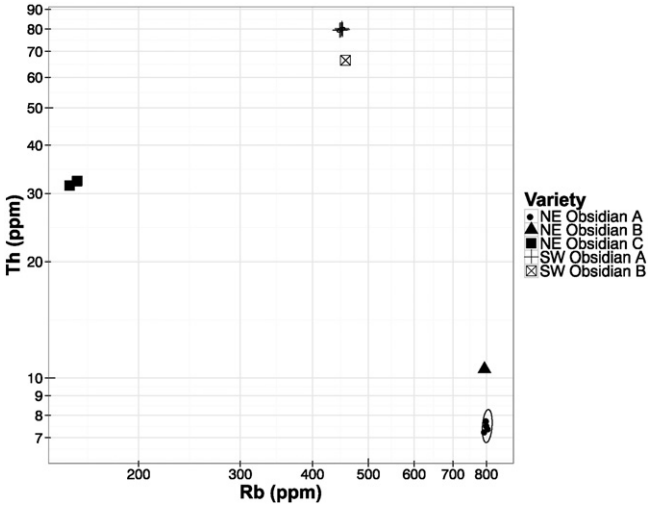

Fig. 3. Bivariate plot of Rb and Th abundances as determined by NAA. Ellipses drawn at the 95% confidence interval around obsidian sources *NE A* and *SW C*. The ellipse around *SW C* is small and partially hidden by the data point symbols.

4.2. Spatial distribution

The spatial distribution of the different varieties of volcanic glass suggests the existence of two discrete and non-overlapping distribution zones. The *NE Obsidian A*, *NE Obsidian B*, and *NE Obsidian C* are found exclusively in the northeastern region of the Plateau, whereas *SW Obsidian A* and *B* occur only in the southwestern region of the Plateau (Table 4).

The *NE Obsidian A* and *NE Obsidian B* varieties are distributed in the northeast region of the Plateau. The largest distance between two sites with *NE Obsidian A* is 947 km (Lava Camp and Jiangxigou 2). Assuming that foragers moved 10 km a day, a figure that is within the range of distances hunter-gatherers cover in a day (Kelly, 1995), a one-way trip between Lava Camp and Jiangxigou 2 would take about 95 days.

The geological source of *NE Obsidian A* is believed to be near the lake of Chibzhang Co, sometimes referred to as Migriggyangzham Tso (N33.42, E90.30, ~5240 masl). This is a dry and barren region (Rhode et al., 2007) where the surface is reported to be scattered with nodules of obsidian ranging from cobble to pebble sizes (Brantingham et al.,

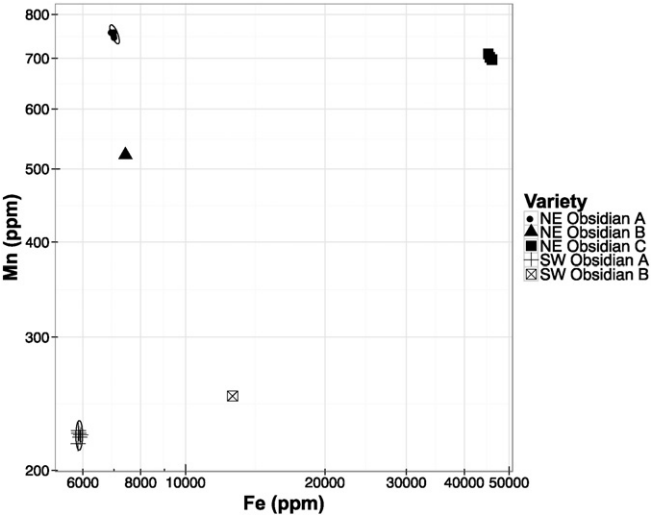

Fig. 4. Bivariate plot of Fe and Mn abundances as determined by NAA. Ellipses drawn at the 95% confidence interval around obsidian sources *NE A* and *SW C*.

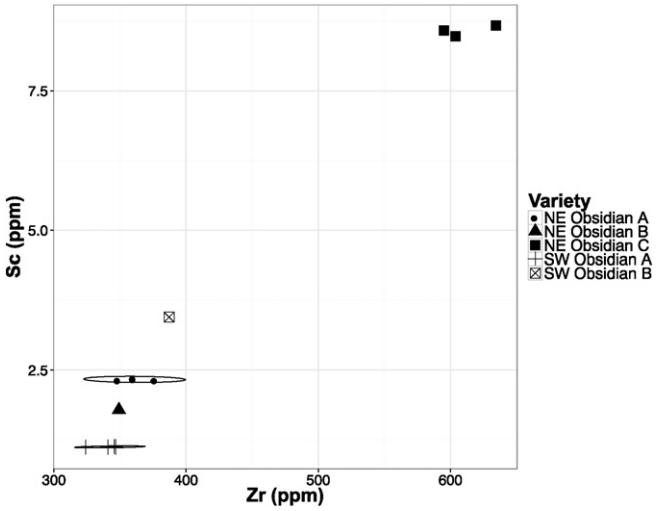

Fig. 5. Bivariate plot of Zr and Sc abundances as determined by NAA. Ellipses drawn at the 95% confidence interval around obsidian sources *NE A* and *SW C*.

2013, Rhode et al., 2007). However, until specimens from Chibzhang Co are characterized using XRF or NAA, we cannot be certain of this. What is more, it is possible that the source of *NE Obsidian* A and *B* is located in the Southwestern region. The distances between Chibzhang Co and the sites containing *NE Obsidian A* range from 150 km to 947 km, averaging 459 km (Table 4). If Chibzhang Co is also the source of *NE Obsidian B*, its presence at Lexie Wudan Co means that it has been transported over 229 km.

The *SW Obsidian A* and *SW Obsidian B* varieties are distributed in the southwest region of the Plateau. The longest distance between two *SW Obsidian A* sites is 526 km (Ngangla Ring Co 10–12 and Su Re), a 52-day trip when moving 10 km a day. *SW Obsidian B* is distributed over a smaller area that overlaps with that of *SW Obsidian A*. The maximum distance between two sites containing *SW Obsidian B* is 112 km (Balung Co and Lopu Kangri 9A). The distance between the geological source of *SW Obsidian B*, Balung Co (N30.59, E83.528, ~5165 masl), and the sites containing *SW Obsidian B* ranges from 27 km to 112 km, with an average of 70 km.

The distances over which obsidian was transported on the Tibetan Plateau are long, but fall within the distribution of lithic raw material transportation distance for hunter-gatherers around the world. Transportation distances of less than 500 km, like the ones of *SW Obsidian A* and *B*, are a common feature of the hunter-gatherer archeological record worldwide (Boulanger et al., 2015, Ellis, 2011, Hoard et al., 1993, Hoard et al., 1992, Holen, 2010, Kilby, 2008, Speer, 2014), and become commonplace in Europe during the Upper Paleolithic (Féblot-Augustins, 1997, Féblot-Augustins, 1999). The two cases of transportation over distances longer than 500 km, between *NE Obsidian A* and its putative source, Chibzhang Co, are impressive, but similar to some of the longest distances reported in other regions of the world. For instance, transportation distances of ~700 km have been recorded in the European Upper Paleolithic record (Féblot-Augustins, 1997, Féblot-Augustins, 1999), and distances ranging from 1000 to 1500 km have also been observed in North America very shortly after humans entered the continent, during the Paleoindian period (Boulanger et al., 2014, Hester et al., 1985, Kilby, 2014, Koldehoff and Loebel, 2013, Tankersley, 1991).

These transportation distances, however, may be the result of different processes that are equifinal (Meltzer and Ellis, 1989). For example, they may represent multiple short foraging moves, but also a few longer moves. Alternatively they may represent direct exchange between pastoralists that occupy the high Plateau and semi-sedentary groups that move up onto the margins of the high Plateau. Such direct exchange may explain why obsidian is relatively rare compared to other types of raw material that are procured directly from geological sources. Finally, obsidian may be transported over long distance through scavenging tool stone from previously occupied sites.

5. Discussion

The distribution of obsidian varieties into two discrete and non-overlapping regions is intriguing. But given the small size of our sample, we cannot draw strong conclusions about the behavioral underpinnings of the distribution of the obsidian varieties. We can, however, offer some hypotheses for the distribution of obsidian varieties into two discrete zones.

The recognition of two distribution zones may be a product of sample size. As mentioned above, many of the archeological sites in our samples were not excavated systematically, and not all the obsidian artifacts were analyzed. We may have thus failed to detect the presence of NE obsidian varieties in the southwestern region, or vice versa.

If the lack of overlap of obsidian varieties between the northeast and the southwest regions of the Plateau is robust to sample size problems, then this would suggest the existence of two obsidian distribution

Table 4
Sources of obsidian and basaltic glass, by site and region. Chibz Co refers to Chibzhang Co. The source of "*Obsidian D*" is also located at Balung Co site.

Site	Region	Variety	Distance from Chibz Co	Distance to Balung Co
Erdaogou	Northeast	*NE Obsidian A*	268 km	–
Jiangxigou 2	Northeast	*NE Obsidian A*	947 km	–
Lava Camp	Northeast	*NE Obsidian A, C*	150 km	–
Lexie Wudan Co	Northeast	*NE Obsidian B*	229 km	–
Police Station 1	Northeast	*NE Obsidian A*	377 km	–
Xidatan 2	Northeast	*NE Obsidian A*	442 km	–
Balung Co	Southwest	*SW Obsidian A, B*	771 km	0 km
Kay Lak Basin 11–3	Southwest	*SW Obsidian B*	–	27 km
Kay Lak Basin 11–4	Southwest	*SW Obsidian A*	–	–
Kay Lak Basin 11–7	Southwest	*SW Obsidian A, B*	–	34 km
Lopu Kangri 13–1	Southwest	*SW Obsidian B*	–	105 km
Lopu Kangri 9A	Southwest	*SW Obsidian B*	–	112 km
Ngangla Ring Co 10–12	Southwest	*SW Obsidian A*	–	–
Ngangla Ring Co 10–14	Southwest	*SW Obsidian A*	–	–
Ngangla Ring Co 10–4	Southwest	*SW Obsidian A*	–	–
Ngangla Ring Co 10–7	Southwest	*SW Obsidian A*	–	–
Paiku Co 2	Southwest	*SW Obsidian A*	–	–
Paiku Co 3	Southwest	*SW Obsidian A*	–	–
Su-Re	Southwest	*SW Obsidian A*	–	–
Tingri 1	Southwest	*SW Obsidian A*	–	–
Zhongba 13–3	Southwest	*SW Obsidian A*	–	–

zones, not unlike the obsidian "conveyance zones" identified in the Great Basin, USA, regions within which distinct suites of toolstone was transported (Beck and Jones, 2011, Connolly, 1999, Goebel, 2007, Graf, 2002, Jones et al., 2003; Jones et al., 2012, Smith, 2005, Smith, 2010).

If real, the two obsidian zones would suggest that the two regions were occupied independently, and that interactions between them may have been limited, at least in terms of transportation or exchange of stone tools. The population structure suggested by the distribution of obsidian varieties may have left a signature in the genetic makeup of contemporary Tibetans, especially if it persisted through a large part of the Holocene, and may explain the genetic distance between contemporary Tibetans from the north and the south of the Plateau (e.g. Kang et al., 2010, Qin et al., 2010).

Present-day pastoralists in Tibet move up river valleys to pastures on the high Plateau in the summer, and back down again to intermountain river valleys in the fall. This mobility pattern may have been one of long standing, and may have been present even during the earliest periods of Tibet's prehistory. The dispersal of obsidian varieties into two discrete distribution zones may thus reflect the utilization of different drainage patterns of different major river systems, such as the Huanghe (Yellow River) in the north, and the Yarlongzangbo (Bhramaputra) River, or Sutlej Rivers in the south. Such a mobility pattern, limited to stream channels, would also have limited movements between the northeastern and the southwestern Tibetan Plateau.

6. Conclusions

We presented here an initial report on the chemical characterization of obsidian artifacts and of one obsidian-source nodule from the Tibetan Plateau. Our results augment our understanding of human activity in the region in several ways, and they help establish the beginnings of a lithic-source database for future studies on the Plateau. We have established that the early inhabitants of the Plateau exploited at least five varieties of volcanic glass. Our analyses suggest that three of these obsidian varieties are represented in archeological assemblages on the northeastern region of the Plateau, whereas previous researchers have identified only one. The geological source areas for these three chemical varieties of obsidian may be near Chibzhang Co (a.k.a., Migriggyangzham Tso); however, this needs to be confirmed with more fieldwork. Chemical compositions for obsidian from the southwestern region of the Plateau are reported here for the first time, and the geological source area for one of these sources has been determined through analysis of an unmodified cobble. Finally, although the exact mode of human mobility and exchange/transportation of toolstone on the Tibetan Plateau remains to be determined, our results may reflect foraging movements hundreds of kilometer long that are comparable to the longest lithic raw material distances observed in other regions of the world.

Acknowledgments

CP, DR, DBM and PJB are funded by the U.S. National Science Foundation (SBE 0214870 and 0841435). JWO is supported by the University of Arizona Je Tsongkhapa Endowment for Central and Inner Asian Archeology, the Henry R. Luce Foundation, and the American Council of Learned Societies. DMH and JQ thank the Comer Science and Education Foundation, as well as Tyler Huth and Lei Guoliang for help in the field. The Archeology Laboratory at MURR is supported in part by a grant from the U.S. National Science Foundation (1415403).

Appendix A. Supplementary data

Supplementary data to this article can be found online at http://dx.doi.org/10.1016/j.jasrep.2015.12.009.

References

Aldenderfer, M., Zhang, Y., 2004. The prehistory of the Tibetan Plateau to the seventh century A.D.: perspectives and research from China and the west since 1950. J. World Prehist. 18, 1–55.

Barton, L.W., Brantingham, P.J., Ji, D.X., 2007. Late Pleistocene climate change and Paleolithic cultural evolution in northern China: implications from the last Glacial maximum. In: Madsen, D.B., Fahu, C., Xing, G. (Eds.), Late Quaternary Climate Change and Human Adaptation in Arid China Evolutionary Archaeology. Elsevier, Amsterdam, pp. 105–128.

Beall, C.M., 2007. Two routes to functional adaptation: Tibetan and Andean high-altitude natives. Proc. Natl. Acad. Sci. 104, 8655–8660.

Beall, C.M., Cavalleri, G.L., Deng, L., Elston, R.C., Gao, Y., Knight, J., Li, C., Li, J.C., Liang, Y., McCormack, M., Montgomery, H.E., Pan, H., Robbins, P.A., Shianna, K.V., Tam, S.C., Tsering, N., Veeramah, K.R., Wang, W., Wangdui, P., Weale, M.E., Xu, Y., Xu, Z., Yang, L., Zaman, M.J., Zeng, C., Zhang, L., Zhang, X., Zhaxi, P., Zheng, Y.T., 2010. Natural selection on EPAS1 (HIF2α) associated with low hemoglobin concentration in Tibetan highlanders. Proc. Natl. Acad. Sci. 107, 11459–11464.

Beall, C.M., Song, K., Elston, R.C., Goldstein, M.C., 2004. Higher offspring survival among Tibetan women with high oxygen saturation genotypes residing at 4,000 m. Proc. Natl. Acad. Sci. U. S. A. 101, 14300–14304.

Beck, C., Jones, G.T., 2011. The role of mobility and exchange in the conveyance of toolstone during the Great Basin Paleoarchaic. In: Hughes, R.E. (Ed.), Perspectives on Prehistoric Trade and Exchange in California and the Great Basin. University of Utah Press, Salt Lake City, pp. 55–82.

Boulanger, M.T., Buchanan, B., O'Brien, M.J., Redmond, B.G., Glascock, M.D., Eren, M.I., 2015. Neutron activation analysis of 12,900-year-old stone artifacts confirms 450–510+ km Clovis tool-stone acquisition at paleo crossing (33ME274), northeast Ohio, U.S.A. J. Archaeol. Sci. 53, 550–558.

Boulanger, M.T., Glascock, M.D., Shackley, M.S., Skinner, C., Thatcher, J.J., 2014. Likely source attribution for a possible Paleoindian obsidian tool from northwest Louisiana. La. Archaeol. 37, 81–88.

Brantingham, P.J., Xing, G., 2006. Peopling of the northern Tibetan Plateau. World Archaeol. 38, 387–414.

Brantingham, P.J., Rhode, D., Madsen, D.B., 2010. Archaeology augments Tibet's genetic history. Science 329, 1467.

Brantingham, P.J., Xing, G., Madsen, D.B., Bettinger, R.L., Elston, R.G., 2004. The initial upper paleolithic at Shuidonggou, Northwestern China. In: Brantingham, J.P., Kuhn, S.L., Kerry, K.W. (Eds.), The Early Upper Paleolithic Beyond Western Europe. University of California Press, Berkeley, pp. 223–241.

Brantingham, P.J., Xing, G., Madsen, D.B., Rhode, D., Perreault, C., van der Woerd, J., Olsen, J.W., 2013. Late occupation of the high-elevation northern Tibetan Plateau based on cosmogenic. Lumin. Radiocarbon Ages Geoarchaeol. 28, 413–431.

Brantingham, P.J., Xing, G., Olsen, J.W., Rhode, D.E., Zhang, H.Y., Madsen, D.B., 2007. A short chronology for the peopling of the Tibetan Plateau. In: Madsen, D.B., Fahu, C., Xing, G. (Eds.), Late Quaternary Climate Change and Human Adaptation in Arid China. Elsevier, Amsterdam, pp. 129–150.

Chen, F.H., Dong, G.H., Zhang, D.J., Liu, X.Y., Jia, X., An, C.B., Ma, M.M., Xie, Y.W., Barton, L., Ren, X.Y., Zhao, Z.J., Wu, X.H., Jones, M.K., 2015. Agriculture facilitated permanent human occupation of the Tibetan Plateau after 3600 B.P. Science 347, 248–250.

Chen, Q.-H., Ge, R.-L., Wang, X.-Z., Chen, H.-X., Wu, T.-Y., Kobayashi, T., Yoshimura, K., 1997. Exercise performance of Tibetan and Han adolescents at altitudes of 3,417 and 4,300 m.

Connolly, T.J., 1999. Newberry Crater: a ten-thousand year record of human occupation and environmental change in the basin Plateau Borderlands. University of Utha, Salt Lake City.

Ellis, C., 2011. Measuring Paleoindian range mobility and land-use in the great lakes/northeast. J. Anthropol. Archaeol. 30, 385–401.

Féblot-Augustins, J., 1997. La circulation des matères premières au Paléolithique. 1. Université de Liège.

Féblot-Augustins, J., 1999. La mobilité des groups paléolithiques. Bull. Mem. Soc. d'Anthropologie Paris 11, 219–260.

Gao, X., Pei, S., Wang, H., Zhong, K., 2004. A report on Paleolithic reconnaissance in Ningxia. North China Acta Anthropol. Sin. 23, 307–325.

Ge, R.L., Chen, Q.H., Wang, L.H., Gen, D., Yang, P., Kubo, K., Fujimoto, K., Matsuzawa, Y., Yoshimura, K., Takeoka, M., et al., 1994. Higher exercise performance and lower VO2max in Tibetan than Han residents at 4,700 m altitude. J. Appl. Physiol. 77, 684–691.

Ge, R.-L., Witkowski, S., Zhang, Y., Alfrey, C., Sivieri, M., Karlsen, T., Resaland, G.K., Harber, M., Stray-Gundersen, J., Levine, B.D., 2002. Determinants of erythropoietin release in response to short-term hypobaric hypoxia. J. Appl. Physiol. 92, 2361–2367.

Glascock, M.D., 1992. Characterization of archaeological ceramics at MURR by neutron activation analysis and multivariate statistics. In: Neff, H. (Ed.), Chemical Characterization of Ceramic Pastes in Archaeology. Prehistory Press, Madison, pp. 11–26.

Glascock, M.D., Ferguson, J.R., 2012. Report on the analysis of obsidian source specimens by multiple analytical methods. Report Submitted to Bruker Instruments, On file at MURR.

Glascock, M.D., Neff, H., 2003. Neutron activation analysis and provenance research in archaeology. Meas. Sci. Technol. 14, 1516–1526.

Goebel, T., 2007. Pre-archaic and early archaic technological activities at Bonneville Eastates Rockshelter: a first look at the lithic record. In: Graf, K.E., Schmitt, D.N. (Eds.), Paleoindian or Paleoarchaic?University of Utah Press, Salt Lake City, Great Basin human ecology at the Pleistocene-Holocene transition, pp. 156–184.

Graf, K.E., 2002. Paleoindian obsidian procurement and mobility in the western great basin. Curr. Res. Pleistocene 19, 87–89.

Groves, B.M., Droma, T., Sutton, J.R., McCullough, R.G., McCullough, R.E., Zhuang, J., Rapmund, G., Sun, S., Janes, C., Moore, L.G., 1993. Minimal Hypoxic Pulmonary Hypertension in Normal Tibetans at 3,658 m.

Hester, T.R., Evans, G.L., Asaro, F., Stross, F.H., Campbell, T.N., Michel, H.V., 1985. Trace element analysis of an obsidian Paleo-Indian projectile point from Kincaid rockshelter. Tex. Bull. Tex. Archaeol. Soc. 56, 143–153.

Hoard, R.J., Bozell, J.R., Holen, S.R., Glascock, M.D., Neff, H., Elam, J.M., 1993. Source determination of white river group silicates from two archaeological sites in the great plains. Am. Antiq. 58, 698–710.

Hoard, R.J., Holen, S.R., Glascock, M.D., Neff, H., Elam, J.M., 1992. Neutron activation analysis of stone from the Chadron formation and a Clovis site on the great plains. J. Archaeol. Sci. 19, 655–665.

Holen, S.R., 2010. The eckles Clovis site, 14JW4: a Clovis site in northern Kansas. Plains Anthropol. 55, 299–310.

Hudson, A.M., Olsen, J.W., Quade, J., 2014. Radiocarbon dating of interdune paleo-wetland deposits to constrain the age of mid-to-late Holocene microlithic artifacts from the zhongba site. Southwest. Qinghai-Tibet Plateau Geoarchaeol. 29, 33–46.

Hudson, A.M., Quade, J., Huth, T.E., Lei, G., Cheng, H., Edwards, L.R., Olsen, J.W., Zhang, H., 2015. Lake level reconstruction for 12.8–2.3 ka of the ngangla ring Tso closed-basin lake system, southwest Tibetan Plateau. Quat. Res. 83, 66–79.

Ji, D., Chen, F., Bettinger, R.L., Elston, R.G., Geng, Z., Barton, L., Wang, H., An, C., Zhang, D., 2005. Human response to the last glacial maximum: evidence from north China. Acta Anthropol. Sin. 24, 270–282.

Jones, G.T., Beck, C., Jones, E.E., Hughes, R.E., 2003. Lithic source use and paleoarchaic foraging territories in the great basin. Am. Antiq. 68, 5–38.

Jones, G.T., Fontes, L., Horowitz, R., Beck, C., Bailey, D.G., 2012. Reconsidering paleoarchaic mobility in the central great basin. Am. Antiq. 77, 351–367.

Kang, L., Li, S., Gupta, S., Zhang, Y., Liu, K., Zhao, J., Jin, L., Li, H., 2010. Genetic structures of the Tibetans and the Deng people in the Himalayas viewed from autosomal STRs. J. Hum. Genet. 55, 270–277.

Kelly, R.L., 1995. The Foraging Spectrum: Diversity in Hunter-Gatherer Lifeways. Smithsonian Institution Press, Washington, D.C.

Khazaee, M., Glascock, M.D., Masjedi, P., Abedi, A., Nadooshan, F.K., 2011. The origins of obsidian tools from Kul tepe, Iran. Int. Assoc. Obsidian Stud. Bull. 45, 14–17.

Kilby, J.D., 2008. An Investigation of Clovis Caches: Content, Function, and Technological Organization. Department of Anthropology, University of New Mexico.

Kilby, J.D., 2014. Direction and distance in Clovis Chaching. In: Huckell, B.B., David Kilby, J. (Eds.), Clovis Caches: Recent Discoveries and New Research. University of New Mexico Press, Albuquerque, pp. 201–216.

Koldehoff, B., Loebel, T.J., 2013. Clovis and Dalton: unbounded and bounded systems in the midcontinent of North America. In: Adams, B., Blades, B.S. (Eds.), Lithic Materials and Paleolithic Societies. Wiley-Blackwell, Oxford, pp. 270–287.

Li, F., Kuhn, S.L., Gao, X., Chen, F.-Y., 2013. Re-examination of the dates of large blade technology in China: a comparison of shuidonggou locality 1 and locality 2. J. Hum. Evol. 64, 161–168.

Madsen, D.B., Jingzen, L., Brantingham, P.J., Xing, G., Elston, R.G., Bettinger, R.L., 2001. Dating shuidonggou and the upper palaeolithic blade industry in north China. Antiquity 75, 706–716.

Madsen, D.B., Oviatt, C.G., Zhu, Y., Brantingham, P.J., Elston, R.G., Chen, F., Bettinger, R.L., Rhode, D., 2014. The early appearance of shuidonggou core-and-blade technology in north China: implications for the spread of anatomically modern humans in northeast Asia? Quat. Int. 347, 21–28.

Meltzer, D.J., Ellis, C.J., 1989. Was stone exchanged among Eastern North American Paleoindians? In: Lothrop, J.C. (Ed.), Eastern Paleoindian Lithic Resource Use. Westview Press, Boulder, pp. 11–39

Neff, H., 2000. Neutron activation analysis for provenance determination in archaeology. In: Ciliberto, E., Spoto, G. (Eds.), Modern Analytical Methods in Art and ArchaeologyChemical Analysis Series. Wiley, pp. 81–134.

Qin, Z., Yang, Y., Kang, L., Yan, S., Cho, K., Cai, X., Lu, Y., Zheng, H., Zhu, D., Fei, D., Li, S., Jin, L., Li, H., 2010. A mitochondrial revelation of early human migrations to the Tibetan Plateau before and after the last glacial maximum. Am. J. Phys. Anthropol. 143, 555–569.

Rademaker, K., Hodgins, G., Moore, K., Zarrillo, S., Miller, C., Bromley, G.R.M., Leach, P., Reid, D.A., Álvarez, W.Y., Sandweiss, D.H., 2014. Paleoindian settlement of the high-altitude Peruvian Andes. Science 346, 466–469.

Rhode, D., Haiying, Z., Madsen, D.B., Xing, G., Jeffrey Brantingham, P., Haizhou, M., Olsen, J.W., 2007. Epipaleolithic/early Neolithic settlements at Qinghai lake, western China. J. Archaeol. Sci. 34, 600–612.

Simonson, T.S., Yang, Y., Huff, C.D., Yun, H., Qin, G., Witherspoon, D.J., Bai, Z., Lorenzo, F.R., Xing, J., Jorde, L.B., Prchal, J.T., Ge, R., 2010. Genetic evidence for high-altitude adaptation in Tibet. Science 329, 72–75.

Smith, G.M., 2005. The Paleoarchaic occupation of moonshine spring south and Moonshadow Spring, Pershing County, Nevada: implications for early-period mobility in the Great Basin. Nev. Archaeol. 57–70.

Smith, G.M., 2010. Footprints across the black rock: temporal variability in prehistoric foraging territories and toolstone procurement strategies in the western great basin. Am. Antiq. 75, 865–885.

Speer, C., 2014. LA-ICP-MS analysis of Clovis period projective points frmo the gault site. J. Archaeol. Sci. 52, 1–11.

Tankersley, K.B., 1991. A geoarchaeological investigation of distibution and exchange in the raw material econonies of clovis groups in Eastern North America. In: Montet-White, A., Holen, S. (Eds.), Raw Material Economies among Prehistoric Hunter-Gatherers. University of Kansas, Lawrence, Kansas, pp. 285–303.

Van Der Woerd, J., Tapponnier, P., Ryerson, J.F., Meriaux, A.-S., Meyer, B., Gaudemer, Y., Finkel, R.C., Caffee, M.W., Guoguan, Z., Zhiqin, X., 2002. Uniform postglacial slip-rate along the central 600 km of the Kunlun fault (Tibet), from 26Al, 10Be, and 14C dating of riser offsets, and climatic origin of the regional morphology. Geophys. J. Int. 148, 356–388.

Wang, B., Zhang, Y.-B., Zhang, F., Lin, H., Wang, X., Wan, N., Ye, Z., Weng, H., Zhang, L., Li, X., Yan, J., Wang, P., Wu, T., Cheng, L., Wang, J., Wang, D.-M., Ma, X., Yu, J., 2011. On the origin of Tibetans and their genetic basis in adapting high-altitude environments. PLoS One 6, e17002.

Yang, Y.H., Fang, J.Y., Pan, Y.D., Ji, C.J., 2009. Aboveground biomass in Tibetan grasslands. J. Arid Environ. 73, 91–95.

Yi, X., Liang, Y., Huerta-Sanchez, E., Jin, X., Cuo, Z.X.P., Pool, J.E., Xu, X., Jiang, H., Vinckenbosch, N., Korneliussen, T.S., Zheng, H., Liu, T., He, W., Li, K., Luo, R., Nie, X., Wu, H., Zhao, M., Cao, H., Zou, J., Shan, Y., Li, S., Yang, Q., Asan, N., Tian, P., Xu, G., Liu, J., Jiang, X., Wu, T., Zhou, R., Tang, G., Qin, M., Wang, J., Feng, T., Li, S., Huasang, G., Luosang, J., Wang, W., Chen, F., Wang, Y., Zheng, X., Li, Z., Bianba, Z., Yang, G., Wang, X., Tang, S., Gao, G., Chen, Y., Luo, Z., Gusang, L., Cao, Z., Zhang, Q., Ouyang, W., Ren, X., Liang, H., Zheng, H., Huang, Y., Li, J., Bolund, L., Kristiansen, K., Li, Y., Zhang, Y., Zhang, X., Li, R., Li, S., Yang, H., Nielsen, R., Wang, J., Wang, J., 2010. Sequencing of 50 human exomes reveals adaptation to high altitude. Science 329, 75–78.